Journal of Molecular Graphics and Modelling 29 (2010) 309–320

Contents lists available at ScienceDirect

Journal of Molecular Graphics and Modelling

journal homepage: www.elsevier.com/locate/JMGM

# DFG-in and DFG-out homology models of TrkB kinase receptor: Induced-fit and ensemble docking

Črtomir Podlipnik[a,b,*], Federico Tutino[b], Anna Bernardi[c], Pierfausto Seneci[b,c]

[a] University of Ljubljana, Faculty of Chemistry and Chemical Technology, Aškerčeva 5, 1000 Ljubljana, Slovenia
[b] Universitá degli Studi di Milano, Center for Biomolecular Interdisciplinary Studies and Industrial Applications (CISI), Via Fantoli 16/15, 20138 Milano, Italy
[c] Universitá degli Studi di Milano, Dipartimento di Chimica Organica e Industriale, via Venezian 21, 20133 Milano, Italy

ARTICLE INFO

*Article history:*
Received 1 June 2010
Received in revised form
14 September 2010
Accepted 16 September 2010
Available online 7 October 2010

*Keywords:*
Kinase inhibitors
DFG-in and DFG-out
TrkB

ABSTRACT

Kinases from the Trk family are important for the regulation of development and for the correct functioning of the neural system. Deregulation (over-expression) of Trks leads to survival and proliferation of different human cancers. Therefore, development of inhibitors for Trks that can disrupt the signal pathway of Trks could lead to cure against cancer as well as to nociception. Homology models built by YASARA have been used as targets for docking various libraries of known Trk inhibitors. The receptor plasticity was compensated with induced fit docking and/or ensemble docking. It was determined that DFG-in and DFG-out conformational states of TrkB kinase must be taken into account in order to get more reasonable relationships between the docking score and the activity measured by $pIC_{50}$ for the corresponding ligands.



## 1. Introduction

Trk (tropomyosin related kinase) receptors are transmembrane proteins belonging to the family of receptor tyrosine kinases (RTKs). Trk receptors exist in three different homologous isoforms: TrkA, TrkB and TrkC. Different growth factors called neurotrophines (NT) are required for the activation of each of those three Trk receptors: namely, TrkA is activated by nerve growth factor (NGF), TrkB is preferentially activated by brain derived neurotrophic factor (BDNF) and neurotrophin NT-4/5, and TrkC is normally activated by neurotrophin NT-3. The structure of each Trk receptor is divided into three regions: an extracellular domain (NT ligand binding), a transmembrane region, and an intracellular kinase domain. The binding of neurotrophic factor to the extracellular domain of Trks causes their autophosphorylation, and consequently triggers downstream signal transduction pathways. An example of such transduction pathway is coupling Trk/BDNF with translational control in dendrites as shown in Fig. 1 [1]. Trks are important for maintenance and survival of neuronal tissue cells during their development in the embryonic phase. There is some reported evidence that Trks are necessary also in the postembryonic phase for the correct functioning of the nervous system, as well as for nociception [2,3]. Several studies have also indicated association of TrkB receptor with Alzheimer's disease [4,5]. Numerous studies have reported some connection between over-expression of Trks outside the central neural system and various types of cancer [6]. Normally, Trks are expressed at low levels outside the central neural system in adults, while pathological over-expression, activation and amplification of Trks are typical for numerous cancers including neuroblastoma [6–9], ovarian [10,11], prostate [12] and colorectal cancer [13]. Thus the interest of the pharmaceutical industry for the discovery and the development of selective inhibitors of Trk receptor kinases that might provide targeted treatments for cancer and pain is not surprising. An excellent review on small-molecule inhibitors of Trk receptor was recently written by Wang et al. [14], reporting many inhibitors that possess excellent *in vitro* potencies and, in some cases, have progressed into clinical trials.

Up to date no high resolution crystallographic structure of the kinase domain of any Trk family member has been deposited in RCSB Protein Data Bank (PDB) [15]. Therefore, researchers are limited to using homology models or surrogate crystal structures for structure-based design of Trk kinase receptor inhibitors.

All kinases have a conserved activation loop, which is important in regulating their activity and is marked by a conserved DFG motif. The activation loop can assume both a conformation that is catalytically competent (DFG-in), and an 'inactive' conformation DFG-out in which the activation loop blocks the substrate binding site. Type-I kinase inhibitors recognize the active, DFG-in conformer, but type-II inhibitors recognize the inactive (DFG-out) conformation, hence both conformer are relevant for drug design purposes.

* Corresponding author at: University of Ljubljana, Faculty of Chemistry and Chemical Technology, Aškerčeva 5, 1000 Ljubljana, Slovenia. Tel.: +386 1 2419 434.
*E-mail address:* crtomir.podlipnik@fkkt.uni-lj.si (Č. Podlipnik).

1093-3263/$ – see front matter © 2010 Elsevier Inc. All rights reserved.
doi:10.1016/j.jmgm.2010.09.008

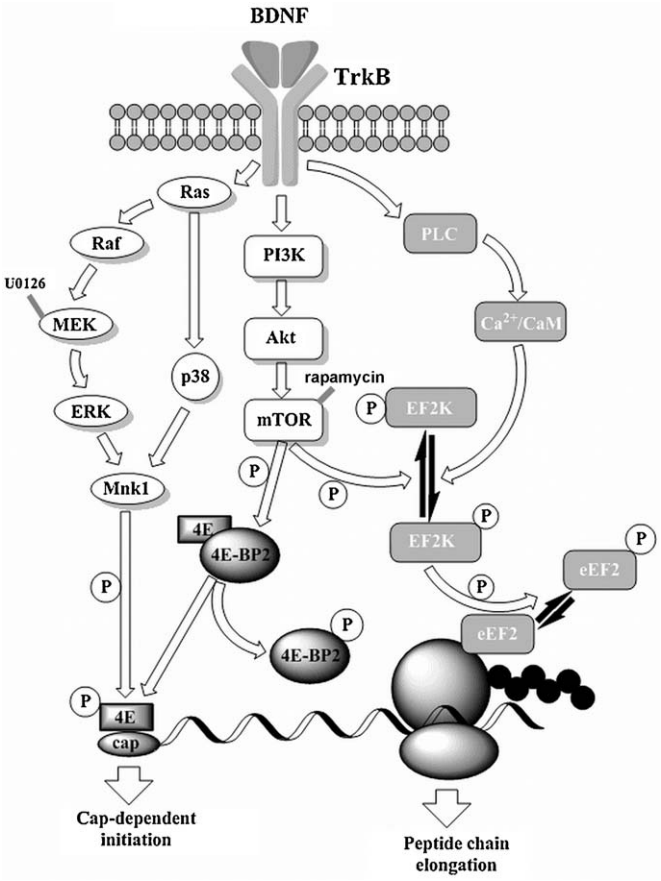


**Fig. 1.** The major signalling pathways coupling TrkB with translation control in dendrites.

Trks, which have a large gatekeeper residue (Phe) and one glycine preceding the DFG (Asp-Phe-Gly) motif, are among the kinases which can adopt both conformations [16,17]. Based on this fact, pharmaceutical industries have built the homology models of TrkA and TrkB kinase domains based on different templates in both DFG-in (active) (AstraZeneca [18]) and DFG-out (inactive) (BMS [19]; Pfizer [20]) conformations.

In this work, we describe the development of a protocol for virtual screening of TrkB inhibitors which could be used for our search of proprietary inhibitors. As we did not find any relevant model of TrkB kinase receptor in PDB, we designed homology models from its aminoacidic sequence. The final models (TrkB:ligand complexes) used in enrichment studies were built with YASARA Structure (homology modelling software) [21,22] and were obtained for both DFG-in and DFG-out conformations. These models were subsequently used in docking studies by Schrödinger's induced-fit docking, known for its ability to reproduce native poses of ligands within their receptor [23]. The models were validated using a set of known Trk kinase inhibitors.

## 2. Methods

### 2.1. Homology modelling of TrkB kinase domain

Since no suitable X-ray structure for TrkB kinase receptor is available in PDB [15], we have used YASARA Structure's homology modelling module [21,22] to build a high resolution model of TrkB from its aminoacidic sequence. YASARA (Yet Another Scientific Artificial Reality Application) is a simple to use, reliable [24] and universal package for molecular graphics, molecular modelling and molecular dynamics. The most sophisticated version of YASARA (YASARA Structure) has also a complete homology modelling module that performs automatically all the steps from aminoacidic sequence (input) to a refined high resolution model (output). YASARA also produces an automatically written, detailed scientific report about individual modelling steps.

As a model sequence for homology modelling we used a protein kinase domain in human Neurotrophic tyrosin kinase receptor type 2 [25], identified as Q16620 in UniProtKB/Swiss-Prot [26–28]. The homology models were obtained using the following protocol: PSI-BLAST [29] integrated in YASARA was run to identify the 15 closest templates in the PDB. The resulting PDB structures with the highest degree of similarity to our target sequence are listed in Table 1.

Then, BLAST was used to retrieve homologous sequences, creating a multiple sequence alignment and feeding it to the 'Discrimination of Secondary structure Class (DSC)' prediction algorithm [30]. Side-chains were built, optimized and fine-tuned in the next step, and all newly modelled parts were subjected to a combined steepest descent and simulated annealing minimization during which the backbone atoms of aligned residues were kept fixed to avoid potential damage. Finally, a fully unrestrained simulated annealing minimization with explicit water was run for the entire model. Some representative homology models of TrkB kinase receptor ranked by theirs Z-score are collected in Table 2.

We selected for further studies and subsequent docking two ligand-protein homology models having a different DFG state. The first model represents a DFG-in conformation of TrkB and is built from a template of insulin receptor tyrosine kinase complexed with an ATP analogue (PDB-ID:1IR3; Table 2-entry 5) [31], and the second model represents an inactive DFG-out conformation of TrkB and is built from a template of insulin receptor tyrosine kinase complexed with a pyrrolopyridine inhibitor (PDB-ID: 3ETA, Table 2-entry 2) [32].

### 2.2. Preparation of ligands

Several different sets of ligands were selected and prepared for docking using Schrodinger's LigPrep (Ligand Preparation) module version 2.3 with default settings [33]. A first set of

**Table 1**
PDB structures showing the highest degree of similarity to Trk-B kinase domain target sequence.

| No. | pdbID | Target coverage | Blast score | Total[a] score | Resol. | Template structure |
|---|---|---|---|---|---|---|
| 1 | 1LUF-A | 93% | 321 | 177.36 | 2.05 | Musk tyrosine kinase |
| 2 | 3EFL-A | 88% | 183 | 160.72 | 2.2 | Vegfr2/motesanib |
| 3 | 3EKK-A | 87% | 270 | 147.91 | 2.1 | Insulin receptor kinase/Inhibitor |
| 4 | 1PI4-A | 87% | 270 | 143.45 | 1.9 | Insulin receptor kinase (catalytic loop mutant) |
| 5 | 3BU3-A | 87% | 262 | 142.62 | 1.65 | Insulin receptor kinase/Irs2 Krlb peptide |
| 6 | 1P4O-A | 87% | 275 | 138.54 | 1.5 | Igf-1R kinase domain (apo unactivated) |
| 7 | 1IR3-A | 89% | 262 | 138.29 | 1.9 | Insulin receptor kinase/peptide substrate and ATP an |
| 8 | 2QOO | 91% | 232 | 137.67 | 1.25 | Human Epha3 kinase (y596f, y602f, y702f) |
| 9 | 3ETA-A | 86% | 273 | 136.52 | 2.6 | Insulin receptor kinase/pyrrolopyridine inhib. |

[a] 'Total score' is the product of the BLAST alignment score, the WHAT_CHECK quality score [1] in the PDBFinder2 database, and the target coverage.

**Table 2**
Five representative homology models of TrkB.

| Entry | Z-score | State | Model ID | Orig #No. | Comment | |
|---|---|---|---|---|---|---|
| 1 | −0.259 | Monomeric | 1LUF-A | 1 | Good | Empty |
| 2 | −0.647 | Monomeric | 3ETA-A04 | 31 | Good | DFG-out |
| 3 | −0.707 | Monomeric | 2QOD-A | 33 | Good | Empty |
| 5 | −0.826 | Monomeric | 1IR3-A01 | 22 | Good | DFG-in |
| 42 | −1.118 | Monomeric | 3EFL-A01 | 2 | Satisfactory | DFG-out |

Z-score is a measure that can tell us how many standard deviations a certain structure is away from the average of standard reference structures. Empty—model of kinase without ligand; DFG-out—model of kinase in DFG-out (inactive) conformation in complex with ligand; DFG-in—model of kinase in DFG-in (active) conformation in complex with ligand.

**Table 3**
Induced fit docking results for selected Trk kinase inhibitors.

| Comp. | DFG-in structures | | DFG-out structures | | [a]DFG | Activity | | [b]Prediction | |
|---|---|---|---|---|---|---|---|---|---|
| | Score[c] | Class | Score[c] | Class | State | $pIC_{50}$ | Class | DFG-state | Activity |
| **1** | −7.2 | 1 | −13.7 (−12.5) | 5 (5) | OUT | 7.74 | 5 | G (G) | G (G) |
| **2** | −10.7 | 3 | −11.6 (−10.4) | 4 (3) | IN | 7.17 | 4 | P (G) | G (S) |
| **3** | −8.9 | 2 | −10.6 (−9.4) | 3 (2) | IN | 7.23 | 4 | P (P) | S (P) |
| **4** | −9.8 | 3 | −10.1 (−8.9) | 3 (2) | IN | 6.37 | 3 | P (G) | G (G) |
| **5** | −10.9 | 3 | −12.1 (−10.9) | 4 (3) | IN | 6.21 | 3 | P (P) | S (G) |
| **6** | −8.6 | 2 | −11.8 (−10.6) | 4 (3) | IN | 6.97 | 4 | P (G) | G (S) |
| **7** | −11.5 | 4 | −12.7 (−11.5) | 5 (4) | IN | 8.1 | 5 | P (P) | G (S) |
| **8** | −10.7 | 3 | −10.6 (−9.4) | 3 (2) | IN | 7.7 | 4 | P (G) | S (S) |
| **9** | −10.7 | 3 | −13.2 (−12.0) | 5 (4) | IN | 7.31 | 4 | P (P) | S (G) |
| **10** | −9.3 | 2 | −11.0 (−9.8) | 3 (3) | OUT | 6.7 | 3 | G (G) | G (G) |
| **11** | −8.0 | 1 | −10.7 (−9.5) | 3 (3) | OUT | 9 | 5 | G (G) | P (P) |
| **12** | −8.1 | 2 | −14.1 (−12.9) | 5 (5) | OUT | 9 | 5 | G (G) | G (G) |
| **13** | −8.9 | 2 | −13.5 (−12.3) | 5 (4) | OUT | 9.57 | 5 | G (G) | G (S) |
| **14** | −11.5 | 4 | −10.1 (−8.9) | 3 (2) | IN | 7.74 | 5 | G (G) | S (S) |
| **15** | −9.9 | 3 | −10.3 (−9.1) | 3 (2) | IN | 7.92 | 4 | P (G) | S (S) |
| **16** | −10.7 | 3 | −12.5 (−11.3) | 5 (4) | ? | 7.33 | 4 | N (N) | S (G) |
| **17** | −9.0 | 2 | −11.7 (−10.5) | 4 (3) | ? | 7 | 4 | N (N) | G (S) |
| **18** | −10.5 | 3 | −13.7 (−12.5) | 5 (5) | ? | 7 | 4 | N (N) | S (S) |
| **19** | −8.6 | 2 | −8.2 (−7.0) | 2 (1) | OUT | 9 | 5 | P (P) | P (P) |
| **20** | −8.3 | 2 | −13.4 (−12.2) | 5 (4) | OUT | 8.3 | 5 | G (G) | G (S) |
| **21** | −9.1 | 2 | −16.7 (−15.5) | 5 (5) | OUT | < 6 | 3 | G (G) | P (P) |
| **22** | −13.7 | 5 | −12.0 (−10.8) | 4 (3) | IN | 7.6 | 4 | G (G) | S (S) |
| **23** | −13.0 | 5 | −11.6 (−10.4) | 4 (3) | IN | 8.52 | 5 | G (G) | G (G) |
| **24** | −9.3 | 3 | −12.5 (−11.3) | 5 (4) | OUT | ? | ? | G (G) | N (N) |

Values in brackets are GlideXP scores corrected by adding a positive offset of 1.2 kcal/mol, an estimation of reorganisation energy associated with the process of binding a ligand to DFG-out structure (see text). The values in brackets in fifth, ninth and tenth columns represents values taking into account correction of GlideXP score for DFG-out structures.

[a] As reported in literature.

[b] In last two columns the ability of using IFD results for prediction of DFG-state and activity is given by G = good; S = satisfactory; P = poor; N = not determined. (?) = not specified.

[c] GlideXP score (kcal/mol).

ligands was composed of 24 Trk kinase inhibitor structures (Fig. 2) reported in the above mentioned review [14] as representative members of several chemotypes (**1**—Amgen, **2**–**9**—Astra Zeneca, **10**—Bayer, **11**–**13**—Bristol-Myers Squibb, **14**, **22**—Cephalon, **15**—GlaxoSmithKline, **16**—Japan Tobacco, **17** and **18**—Johnson & Johnson, **19**, **20**, **24**—Pfizer, **21**—Plexxicon, **23**—Fermentek) with promising *in vitro* activity. When this study was started the majority of available $IC_{50}$ data were obtained for TrkA, a Trk isoform which shares a high degree of similarity with TrkB, most of the data shown in Fig. 2 are referred to TrkA. However, it was recently reported that in many cases TrkA $IC_{50}$s and TrkB $IC_{50}$s are in the same range [18]. A second set of 151 ligands, whose structures and corresponding inhibitory activities are reported as supplementary information, was collected from references mentioned in the same review [14]. A third ligand set made by 1000 "drug-like" ligand decoys selected from a one million compound library was taken from Schrödinger and was used for Glide enrichment studies [34,35].

### 2.3. Induced fit docking

Two YASARA's homology models, one for the DFG-in (1IR3-A01) and one for the DFG-out (3ETA-A04) conformation of TrkB kinase domain, were selected as initial receptor structures for induced-fit docking (IFD). Ligands listed in Fig. 2 were selected for IFD, as provided by Schrödinger Inc. [33,36], a multistep protocol that introduces some protein receptor site plasticity during the process of ligand docking to a corresponding receptor. Initially, ligands were docked to the rigid receptor model using Glide [36,37] with a scaling factor of 0.5 for van der Waals radii for both the ligands and the receptor. In the second step, up to 20 poses for each of these "soft" docked ligands were used to sample protein plasticity using the Prime module within the Schrödinger suite. This sampling includes a conformational search with subsequent minimization, in which only the receptor site residues that have at least one atom within a 5 Å from each ligand were considered. Residues outside the shell were held fixed. As a result, the Prime models of up to 20 new different ligand–receptor complexes have been obtained for each ligand. In the third step, re-docking with the default "hard" van der Waals potential function was performed for all complexes from the second step, and the Glide XP (extra precision) score was used for scoring all docking calculations. A final set of 375 DFG-in and 345 DFG-out complexes of TrkB kinase receptor with their bound ligands was obtained as a result. This method afforded very good results in classifying the

set of ligands for this experiment. However, the IFD process is computationally intensive and time consuming, and it is not an ideal solution when one needs to perform docking calculations on ligand sets exceeding thousands of compounds. For this type of calculations an alternative procedure, making use of ensemble docking [34], was also explored as it is described in the following section.

### 2.4. Ensemble docking and enrichment study

Another option to introduce receptor site plasticity was to take into account several conformational states of the receptor site, an approach known as "ensemble docking" [34]. Four DFG-in and four DFG-out complexes of TrkB kinase receptor with their bound ligand were selected from the results of induced-fit docking calculations.

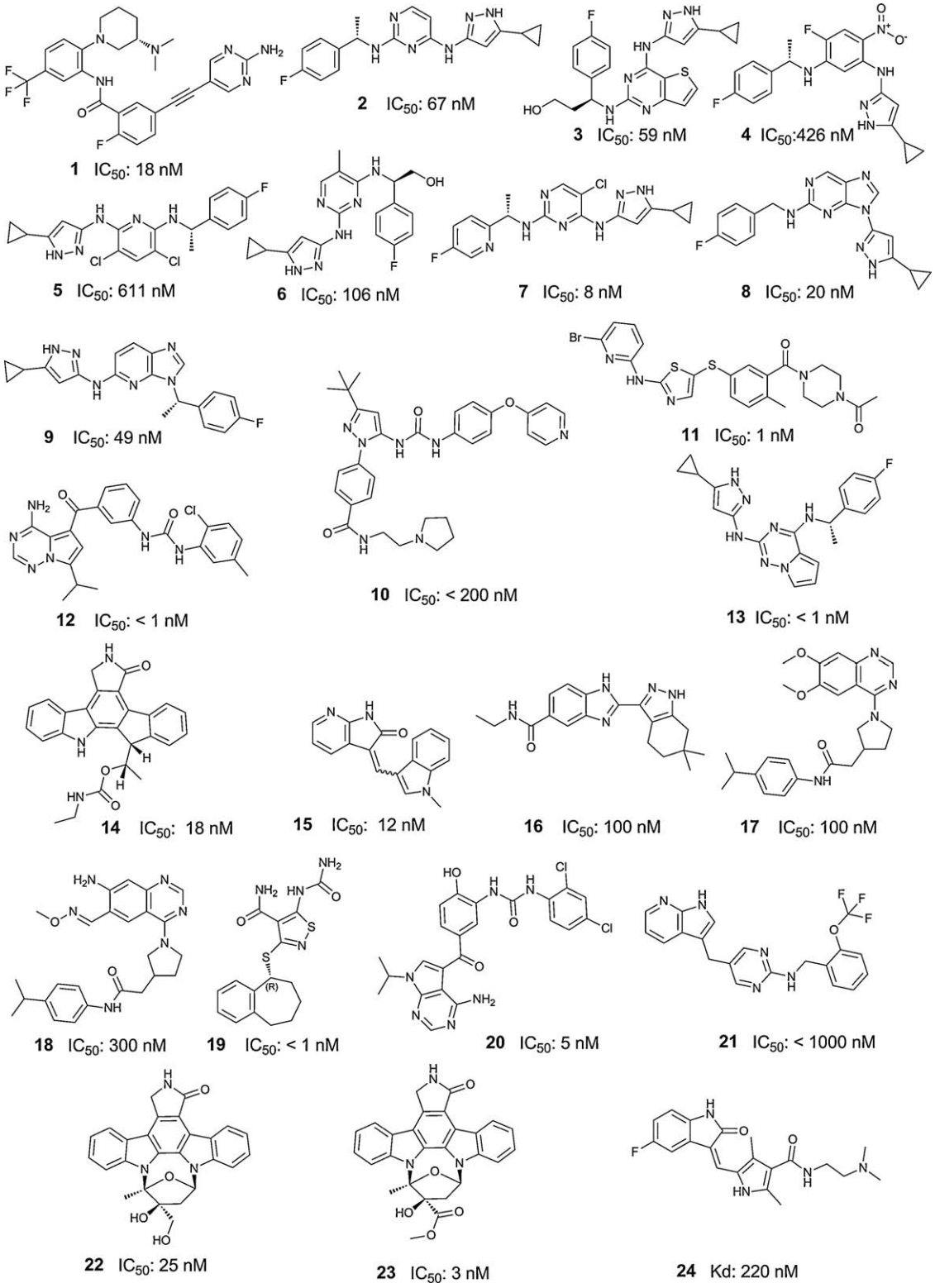


**Fig. 2.** First ligand set. Trk inhibitors from Ref. [14].

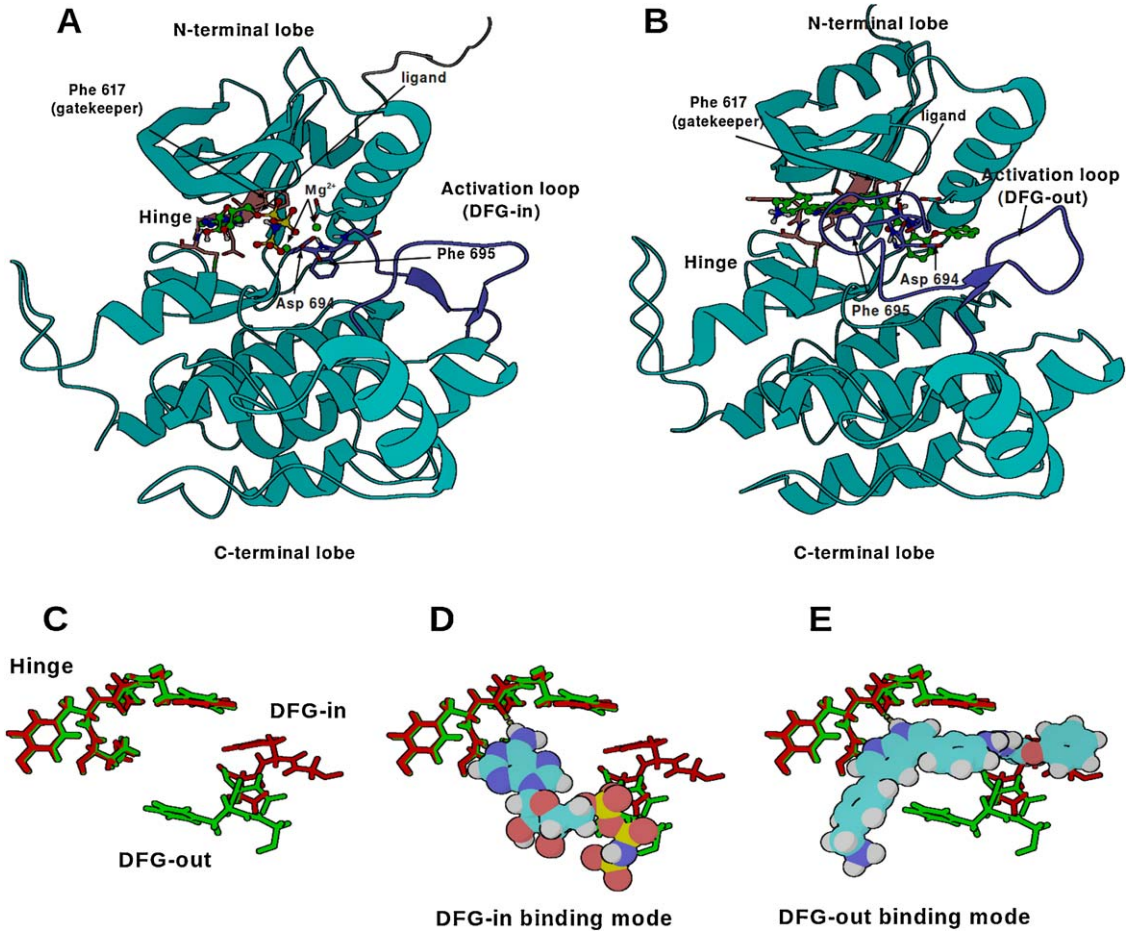


**Fig. 3.** Homology models for TrkB kinase receptor. (A) DFG-in (active form) model based on phosphorylated insulin receptor tyrosine kinase complexed with an ATP analogue (PDB-ID: 1IR3); (B) DFG-out (inactive form) model based on insulin receptor complexed with a pyrrolopyridine inhibitor (PDB-ID: 3ETA); (C) main differences between DFG-in (red) and DFG-out (green) conformations; (D) close view of DFG-in (red) binding mode of an ATP analogue; (E) close view of DFG-out (green) binding mode of a pyrrolopyridine inhibitor.

The selection criteria for the complexes were mainly based on their IFD score and DFG-State as reported in Table 3. Selected complexes were used to generate Glide grids needed for ensemble docking. Schrödinger's Virtual Screening Workflow (VSW) was used to dock the ligand sets described above (see Section 2.2) to the ensemble of multiple TrkB kinase conformations. This virtual screening protocol allows to streamline sets of calculations of increasing accuracy, going from HTVS through SP to XP. All ligands were conserved from one stage to the next. Flexible docking was performed in stages Glide HTVS and Glide SP. The poses obtained in the Glide SP stage were refined in the final Glide XP stage.

The ability of the ensemble docking protocol to retrieve actives from the combined ligand set containing actives and decoys was tested within an enrichment experiment. The used VSW settings were similar to the case of ensemble docking experiment, the only difference was that in enrichment experiment for each ligand only the best pose (minimum score) obtained with docking to eight TrkB targets was retained. The enrichment plot was obtained by plotting the percentage of known ligands recovered ($y$-axis) from the top ranked subset of all screened compounds ($x$-axis/logarithmic scale).

## 3. Results and discussion

### 3.1. Homology modelling study

A DFG-in and a DFG-out model obtained with the homology modelling module of YASARA are presented in Fig. 2. We used both DFG-in and DFG-out models for docking to get a more balanced overview of binding modes to Trk kinase inhibitors.

It is known that the enzymatic activity of kinases strongly depends on their conformational state, which is regulated by phosphorylation of the so-called activation loop. The DFG-in conformation, where Asp694 from the DFG motif is pointing towards the binding site forming a complex with magnesium ion together with ATP γ-phosphate, is necessary for successful enzymatic reaction (Fig. 3A). This interaction is specific for type I inhibitors, i.e. ATP mimics defined as those that bind in and around the "adenine" region. Such inhibitors typically form one to three hydrogen bonds with the kinase's hinge region. Some kinases may also adopt special inactive DFG-out conformations where Phe695 and Asp694 residues from the DFG motif are flipped by 180° from their reference position in the DFG-in active form (Fig. 3B). Recently, many inhibitors referred to as type-II inhibitors and binding to DFG-out conformation were developed [16,17]. These type-II kinase inhibitors occupy a hydrophobic site, that is directly adjacent to the ATP binding pocket, created by a unique DFG-out conformation of the activation loop in which DFG's Phe moves more than 10 Å from its reference position in kinase active conformations (Fig. 3C). Type-II inhibitors trap their target kinases in a DFG-out (inactive) state and exploit a hydrophobic pocket adjacent to the ATP binding site (Fig. 3E). Another important feature of type-II inhibitors is that amino acids surrounding the hydrophobic (allosteric) pocket are less conserved than those that form the ATP binding pocket. Thus, it was suggested that it

may be easier to achieve kinase selectivity with type II ligands [16].

### 3.2. Induced fit docking study

Two different homology models representing an active form (DFG-in, type I, first model) of TrkB kinase receptor and an inactive form (DFG-out, type II, second model) of the same receptor were used. Up to 20 ligand–receptor complexes were obtained as a result for each ligand screened against its kinase receptor. IFD results and lowest Glide-XP scores for each screened ligand are shown in Table 3.

A direct comparison in terms of Glide score between ligands bound to DFG-in and DFG-out receptor structures is difficult due to the higher receptor reorganization energy associated with binding to the DFG-out structures [34]. To get more relevant comparison, the reorganisation energy could be added as a positive offset to the Glide score for ligands docked into DFG-out structures. We estimated this energy by the difference between average value of top four scored DFG-in (**7**, **14**, **22**, **23**) and DFG-out (**1**, **12**, **13**, **20**) IFD complexes with activity measured by $pIC_{50}$ higher than 7.5. The average value of top four GlideXP scores for DFG-in and DFG-out receptors is −12.5 kcal/mol and −13.7 kcal/mol, respectively. Therefore, an estimate of reorganisation energy associated with binding to DFG-out receptor is 1.2 kcal/mol. This value is in agreement with the results of similar studies reported in the literature [34]. GlideXP score corrected for receptor reorganisation energy for DFG-out structures are in brackets in Table 3 and text bellow.

**Table 4**
Classification of ligands by score[a] obtained with IFD and *in vitro* activity measured by $pIC_{50}$.

| Ligand class | Classification by IFD score | Classification by $pIC_{50}$ |
|---|---|---|
| Class 1 | Score > −8.0 | $pIC_{50} < 4.5$ |
| Class 2 | $-8.0 \leq$ score $< -9.5$ | $4.5 \geq pIC_{50} < 5.5$ |
| Class 3 | $-9.5 \leq$ score > −11.0 | $5.5 \geq pIC_{50} < 6.5$ |
| Class 4 | $-11.0 \leq$ score > −12.5 | $6.5 \geq pIC_{50} < 7.5$ |
| Class 5 | Score $\leq -12.5$ | $pIC_{50} \geq 7.5$ |

[a] GlideXP score (kcal/mol).

For an easier comparison between the docking scores of each ligand and its corresponding inhibitory activity reported by $pIC_{50}$, we have distributed ligands into five classes, following a scheme described in Table 4.

We propose some criteria for checking the correlation between the docking score of each ligand and its $pIC_{50}$. The correlation is good if the best ligand's DFG-in or DFG-out score is in the same class

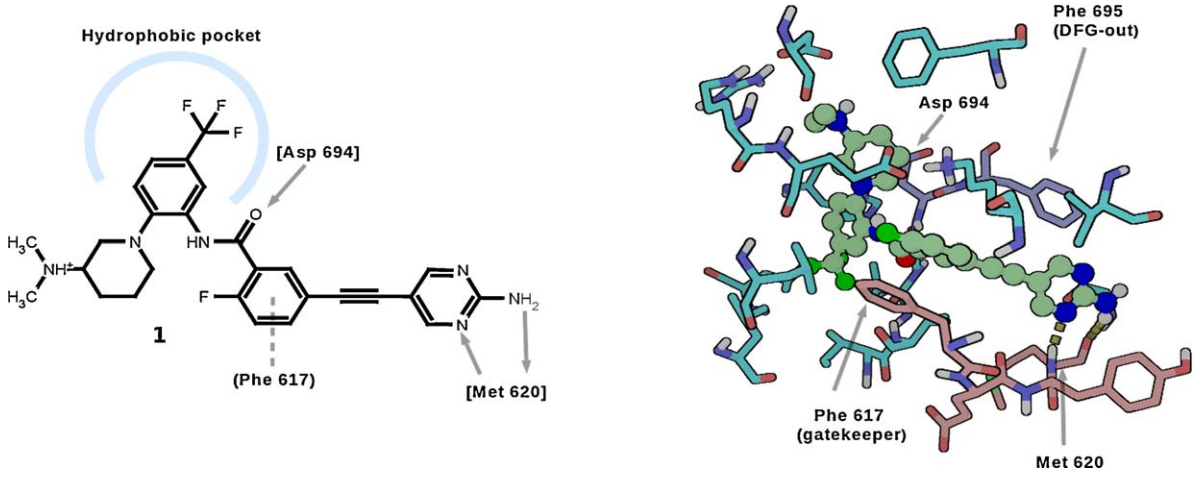


**Fig. 4.** **1**—DFG-out TrkB kinase complex. Gray red—hinge; gray blue—DFG motif; gray green—ligand. (For interpretation of the references to color in this figure legend, the reader is referred to the web version of the article.)

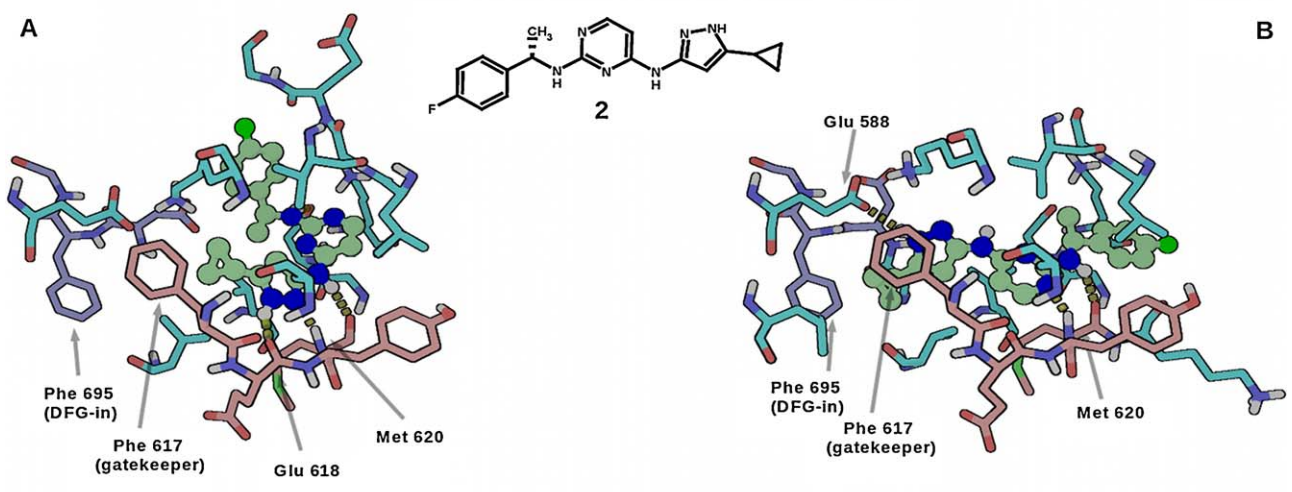


**Fig. 5.** Different binding modes of pyrazolopyrimidine **2**. (A) Binding with hinge via amino-pyrazole. (B) Binding with hinge via amino-pyrimidine. Gray red—hinge; gray blue—DFG motif; gray green—ligand. (For interpretation of the references to color in this figure legend, the reader is referred to the web version of the article.)

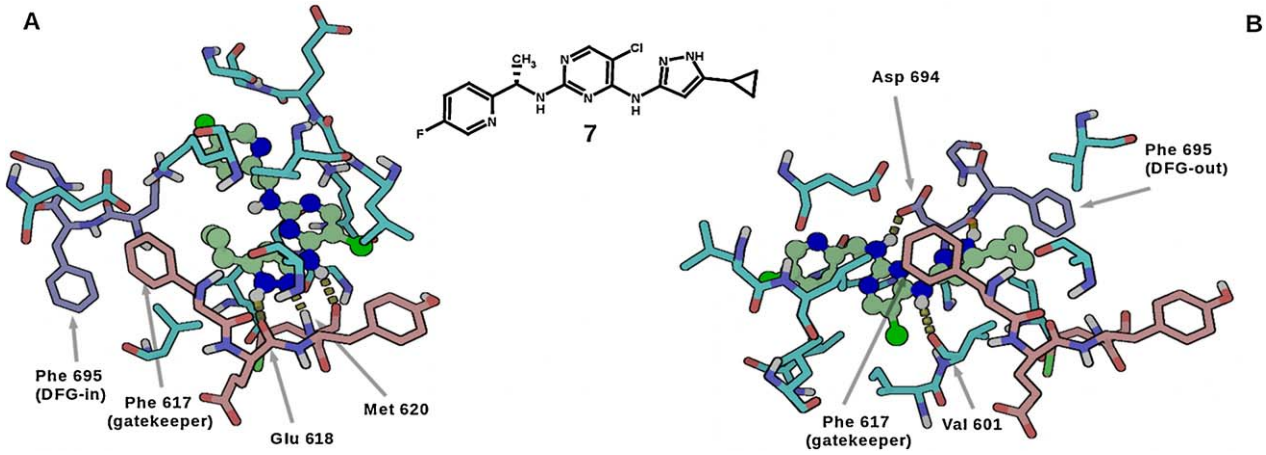


**Fig. 6.** DFG-in (A) and DFG-out (B) binding modes of **7**. Gray red—hinge; gray blue—DFG motif; gray green—ligand. (For interpretation of the references to color in this figure legend, the reader is referred to the web version of the article.)

than its $pIC_{50}$, i.e. if theoretical and experimental data are aligned. If score and $pIC_{50}$ differ by no more than one class, the correlation is defined as satisfactory, while if the difference is more than one class, correlation is defined as bad.

The best scores obtained for each ligand in the DFG-in and DFG-out model might be used as a descriptor to define which type of inhibitor (type I or type II) the ligand may be. If the DFG-in score is lower than the DFG-out one, we may conclude that the ligand binds as an ATP mimic (DFG-in, type I inhibitor), while if the opposite is true, we may assume that the ligand is a DFG-out, type II inhibitor. In general, we observed a big difference between DFG-out and DFG-in score for inhibitors classified as type II (for example, docking results of compounds **1**, **12**, **13**, **20**, and **21** in Table 3). This difference is generally smaller for type I inhibitors (for example, compounds **8**, **14** in Table 3). Moreover, many inhibitors reported in literature as type I have lower DFG-out than DFG-in score (for example compounds **2**–**7**, **9**, **15**). This could mean that type I inhibitors may also be able to interact with the DFG-out conformation of their kinase receptor, while the interaction of type II ligands with DFG-in conformations is less likely. This finding is supported by examples found in literature [16]. Additionally, we noticed that the addition of a positive offset of 1.2 kcal/mol as a contribute of the receptor reorganisation energy to all DFG-out scores improves the prediction of DFG-state using our strategy. Compounds **2**, **4**, **7**, **8** and **15** may be classified as type I inhibitors if we take into account the above mentioned correction of DFG-out scores. Overall, we believe that these examples show how IFD may be useful with some *caveat*, for the classification of kinase inhibitors.

Some interesting complexes between inhibitors and TrkB, obtained with the IFD procedure, are described in the next pages.

Compound **1**, a heteroaryl-substituted alkyne from Amgen, is reported as a nanomolar inhibitor against kinases such as Tie-2 and TrkA [38]. It is also reported to bind to the inactive type II, DFG-out form of kinases [14]. The DFG-in and DFG-out scores (−7.2 kcal/mol vs. −13.7 (−12.5) kcal/mol) obtained in our study suggest that this inhibitor interacts preferentially with the DFG-out form of TrkB. The complex between **1** and the DFG-out conformation of TrkB is shown in Fig. 4, where two hydrogen bond interactions between the heteroaryl group of **1** with the hinge (backbone of Met 620) can be observed. Hydrogen-bonding interaction between the carbonyl oxygen of **1** and the backbone NH of Asp694 (DFG motif), and π–π stacking interaction between gatekeeper Phe617 and an aromatic ring of **1** are also relevant (Fig. 4).

The docked model of pyrazolopyrimidine 2, a potent Trk type I inhibitor developed by Astra Zeneca [39], with the TrkB receptor in an active (DFG-in) conformation is shown in Fig. 5. Literature

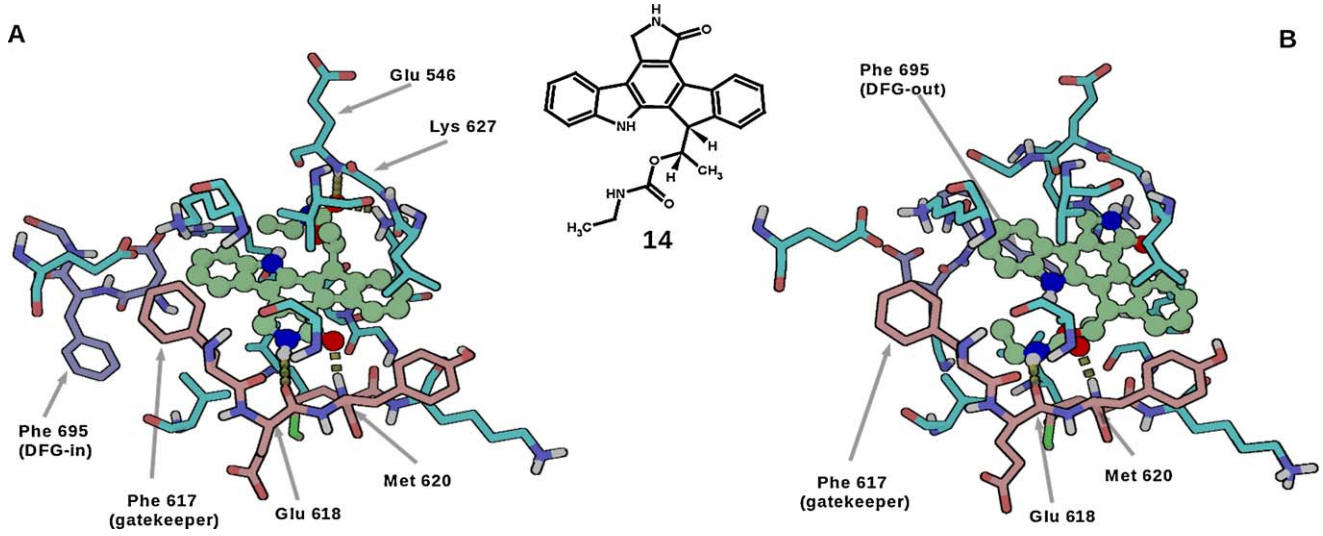


**Fig. 7.** DFG-in (A) and DFG-out (B) complexes between **14** and TrkB. Gray red—hinge; gray blue—DFG motif; gray green—ligand. (For interpretation of the references to color in this figure legend, the reader is referred to the web version of the article.)

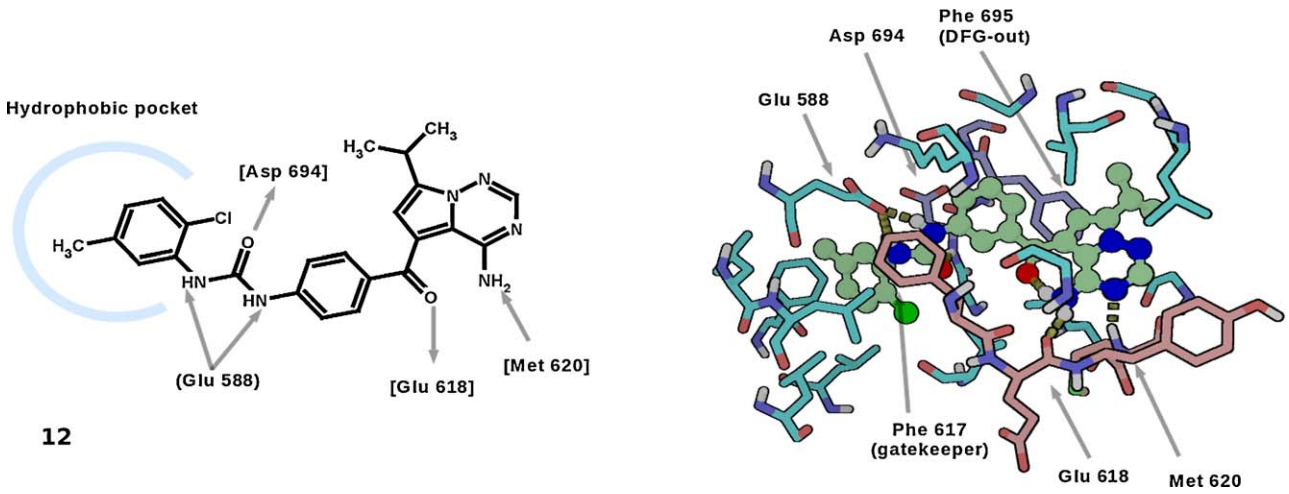


**Fig. 8.** Docking pose of **12** with a DFG-out conformation of TrkB kinase receptor. Gray red—hinge; gray blue—DFG motif; gray green—ligand. (For interpretation of the references to color in this figure legend, the reader is referred to the web version of the article.)

reports that similar compounds could have two binding modes with the hinge region of kinases, either through the amino-pyrazole ring (Fig. 5A) or through the amino-pyrimidine ring (Fig. 5B) [14]. Our results favour DFG-in binding through the pyrazole ring, in agreement with the results of a similar study with a homology TrkB model and as also supported by the crystal structure of a complex between CDK2 and a similar compound [17].

Compound **7**, also from AstraZeneca, has similar GlideXP scores both for DFG-in and DFG-out conformations of TrkB. The compound is reported to be a type I-DFG-in inhibitor, to have low nanomolar potency against TrkA and to inhibit phosphorylation in an MCF10a-TrkADel cellular assay at 1 nM [18]. The complex of **7** with the DFG-in conformation of TrkB is shown in Fig. 6A, with the DFG-out conformation of the same kinase in Fig. 6B. In the DFG-in complex, we observe that **7** is tightly bound to the hinge region with three hydrogen bonds, and the cyclopropyl moiety is facing gatekeeper Phe617 in this way establishing CH-$\pi$ (hydrophobics) interactions. In the DFG-out complex, hydrogen-bonding interactions with the hinge region are not observed, while **7** forms three hydrogen bonds with Asp694 in the DFG motif (two with the backbone, one with side chains) and one with Val601 (backbone). We may conclude that **7** might interact with TrkB also as a type II inhibitor, and therefore kinase's inhibition in both DFG states could be one of the important reasons for its significant *in vivo* activity [18].

Another interesting example is compound **14**, developed by Cephalon as an inhibitor of TrkA ($IC_{50}$ = 18 nM) with good selectivity against PKC, FGFR and KDR [40]. The two IFD complexes of compound **14** with the two homology models of TrkB kinase are shown in Fig. 6. In the DFG-in complex (Fig. 7A) the lactam moiety of **14** forms two hydrogen bonds with the hinge's backbone, and additional hydrogen bond interactions are observed between the carbonyl group of the carbamate in **14** and the Glu546 backbone from the kinase P-loop region. In the DFG-out complex (Fig. 7B) the orientation of **14** is reversed (180° rotation); the acyclic tail is connected with the hinge region by two hydrogen bonds from the carbamate NH, while the carbonyl lactam makes hydrogen-bonding contact with Lys627 side chain. It is well documented in literature that indolocarbazoles similar to **14** typically bind to the hinge region of TrkA kinase through the lactam indolone moiety [40]. This is in agreement with our results as the comparison of

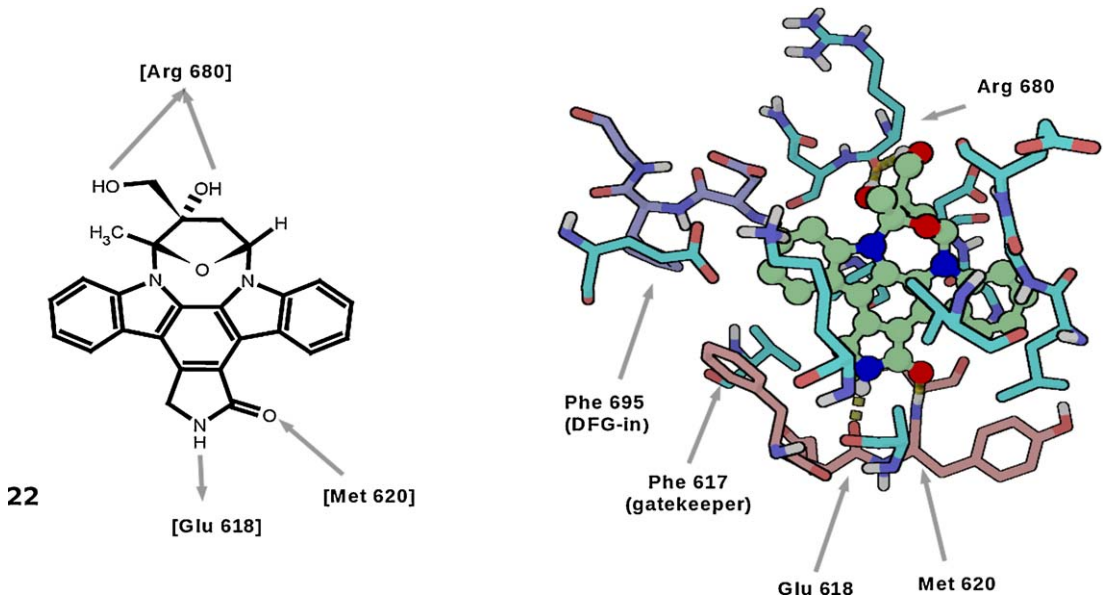


**Fig. 9.** Docking pose of lestaurtinib **22** (type I inhibitor) complexed into the DFG-in conformation of TrkB kinase. Gray red—hinge; gray blue—DFG motif; Gray green—ligand. (For interpretation of the references to color in this figure legend, the reader is referred to the web version of the article.)

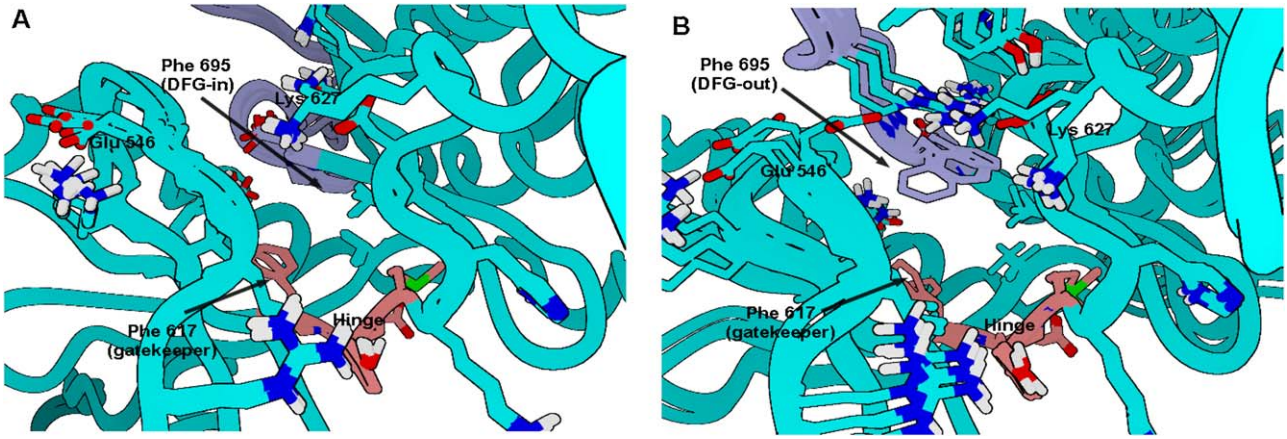


**Fig. 10.** Superposition of ensembles of DFG-in (A) and DFG-out (B) TrkB structures used in ensemble docking experiment.

Glide scores from Table 3 showed that **14** is a more likely DFG-in (−11.5 kcal/mol) than DFG-out (−10.1 (−8.9) kcal/mol) inhibitor.

The docking pose of pyrrolotriazine **12** from Bristol-Myers Squibb, a typical type II—DFG-out Trk and Flt-3 kinase inhibitor [41], is shown in Fig. 8. The inhibitor forms two hydrogen bonding contacts with the hinge region through its 4-amino moiety and 3-nitrogen atom on the ring. Binding is also supported by hydrogen bonding interactions of the urea fragment with the backbone of Asp694 from the DFG motif and the side chain of Glu588. The chloromethylphenyl ring deeply penetrates into the hydrophobic pocket adjacent to the adenine binding site, and is thus responsible for kinase's selectivity. IFD results (min DFG-out Glide XP score = −14.0 (−12.8) kcal/mol, min DFG-in Glide XP score = −8.0 kcal/mol) indicate that **12** is an effective type II inhibitor with very good potency ($IC_{50}$ = 1 nM) against the TrkB kinase receptor.

Another interesting example is provided by lestaurtinib (CEP-701, **22**) a typical type I-DFG-in inhibitor. Lestaurtinib is an orally available small-molecule tyrosine kinase inhibitor with selectivity for FLT3, TrkA, TrkB and TrkC over other kinases [42,43]. Low nanomolar $IC_{50}$s are reported for these kinases, while the IFD results (min DFG-in Glide XP score = −13.7 kcal/mol, min DFG-out Glide XP score = −12.1 (−10.9) kcal/mol) indicate type I vs. type II inhibitor preference. The **22**-DFG-in complex is shown in Fig. 9.

### 3.3. Ensemble docking and enrichment study

IFD is a useful tool for the introduction of receptor plasticity, so that ligand docking may be more realistically modelled than by using only rigid receptor models. On the other hand, IFD is computationally very intensive and time consuming, and thus it is not practically useful for virtual screening of large compound libraries. To overcome these IFD limitations and to retain some receptor plasticity, we docked a series of compounds to "ensembles" of receptor models. We composed two ensembles, each from four representative receptor models obtained from IFD. The first ensemble stems

**Table 5**
Ensemble docking results of ligands **1**–**24** to different models of TrkB obtained with homology modeling and subsequent IFD. Values in bold are minimum value of Glide XP score of DFG-in (DFG-out) models.

| Comp. | GlideXP score (kcal/mol) DFG-IN models | | | | GlideXP score (kcal/mol) DFG-OUT models[a] | | | | DFG | Activity |
|---|---|---|---|---|---|---|---|---|---|---|
| | IN1 | IN2 | IN3 | IN4 | OUT1 | OUT2 | OUT3 | OUT4 | State[b] | $pIC_{50}$ |
| **1** | −4.2 | −5.5 | **−6.9** | −5.2 | – | −9.0 | **−11.6** | −8.5 | OUT | 7.74 |
| **2** | −9.4 | −11.0 | **−11.1** | −8.5 | **−11.5** | −6.6 | −9.4 | −5.9 | IN | 7.17 |
| **3** | −11.7 | **−12.4** | −7.0 | −12.0 | −9.6 | −7.9 | **−14.9** | −5.7 | IN | 7.23 |
| **4** | −8.7 | **−11.6** | −10.3 | −7.8 | −8.3 | −8.4 | **−9.4** | −6.8 | IN | 6.37 |
| **5** | −9.7 | −6.8 | **−10.6** | −6.5 | −8.2 | −6.9 | **−9.2** | −3.8 | IN | 6.21 |
| **6** | **−10.0** | −7.2 | −10.0 | −8.6 | −9.8 | −8.9 | −11.6 | **−11.9** | IN | 6.97 |
| **7** | −7.3 | **−12.3** | −8.1 | −7.2 | −10.4 | −8.2 | **−11.5** | −6.1 | IN | 8.1 |
| **8** | −10.5 | **−11.3** | −7.0 | −9.9 | −8.4 | −8.4 | −8.2 | **−8.8** | IN | 7.7 |
| **9** | −9.2 | **−11.2** | −9.6 | −9.1 | −9.1 | −10.1 | **−12.8** | −9.9 | IN | 7.31 |
| **10** | −7.9 | – | **−7.9** | −3.2 | – | **−12.0** | −11.1 | −6.3 | OUT | 6.7 |
| **11** | **−9.9** | −8.6 | −6.7 | −8.2 | −4.4 | **−9.9** | −6.8 | −9.8 | OUT | 9 |
| **12** | **−7.6** | −6.7 | −3.1 | −5.3 | −8.7 | **−14.7** | −8.5 | −5.0 | OUT | 9 |
| **13** | **−11.2** | −7.6 | −10.4 | −7.7 | −8.6 | −8.5 | −9.7 | **−10.1** | OUT | 9.57 |
| **14** | −6.6 | −6.7 | **−12.8** | −11.9 | **−7.0** | – | −6.5 | – | IN | 7.74 |
| **15** | **−10.2** | −8.9 | −9.8 | −7.0 | −10.8 | −10.1 | −8.2 | **−11.2** | IN | 7.92 |
| **16** | **−12.8** | −12.0 | −11.9 | −11.0 | −13.3 | −13.0 | −8.1 | **−13.6** | ? | 7.33 |
| **17** | −8.3 | −6.7 | −7.6 | −8.0 | −13.2 | **−13.9** | −8.8 | −9.9 | ? | 7 |
| **18** | −7.1 | −7.1 | −7.4 | −8.4 | −12.8 | **−13.3** | −8.7 | −5.8 | ? | 7 |
| **19** | −6.2 | −5.8 | **−8.6** | −7.9 | **−7.5** | −5.0 | −5.7 | −4.4 | OUT | 9 |
| **20** | −6.6 | −3.4 | **−8.4** | −7.4 | −9.0 | **−14.4** | −7.6 | −5.5 | OUT | 8.3 |
| **21** | **−10.5** | −9.2 | −9.7 | −6.4 | **−17.4** | −16.0 | −13.7 | −10.4 | OUT | > 6 |
| **22** | **−14.0** | – | −14.0 | −12.8 | – | **−8.9** | −5.7 | – | IN | 7.6 |
| **23** | −13.7 | −12.6 | **−13.8** | −12.9 | – | **−8.0** | −7.4 | – | IN | 8.52 |
| **24** | **−10.0** | −8.3 | −8.3 | −7.1 | −9.0 | −9.9 | −10.2 | **−13.6** | OUT | ? |

(?) = not specified; (−) = not determined.

[a] If one needs corrected values of DFG-out score, the positive offset of 1.2 kcal/mol need to be added to listed DFG-out scores.

[b] As reported in literature.

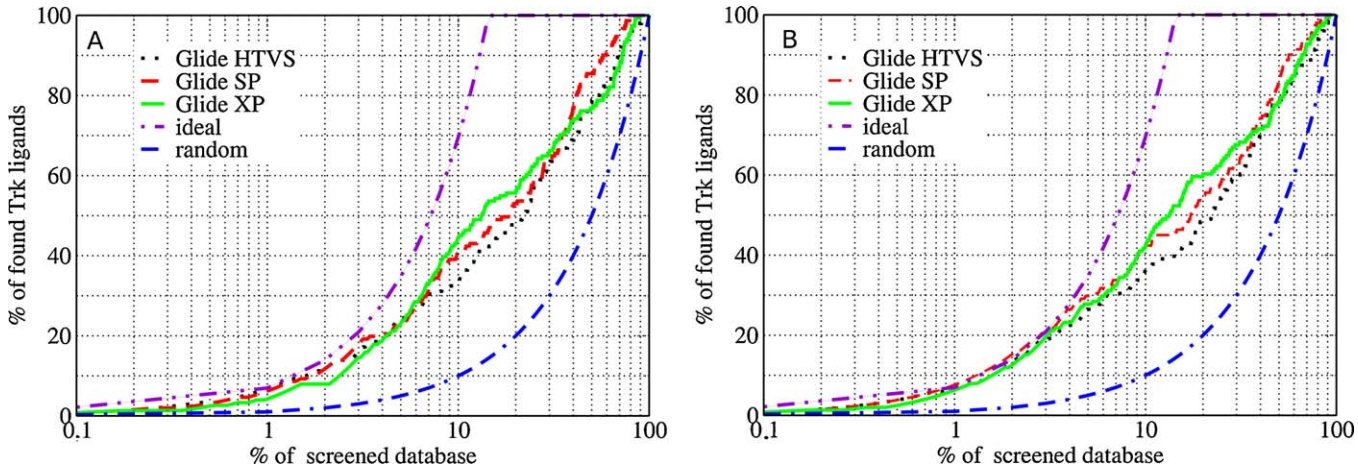


**Fig. 11.** Enrichment graphs for Trk ligands. (A) DFG-out results are not corrected. (B) DFG-out results are corrected by applying a positive offset of 1.2 kcal/mol. *x*-Axis is in logarithmic scale. The ideal curve represents the case when all 151 actives are at the top 151 places of ranked database. The random curve represents the case when actives are randomly distributed over the whole database.

from models based on complexes between the TrkB in DFG-in (active) conformation and type I inhibitors (IN1—lestaurtinib **22**, IN2—compound **7**, IN3—K252A **23**, IN4—compound **14**); the second ensemble stems from models based on complexes between the TrkB in DFG-out (inactive) conformation and type II inhibitors (OUT1—compound **21**, OUT2—compound **12**, OUT3—compound **1**, OUT4—compound **24**). The superimposed structures of each ensemble are represented in Fig. 10 (DFG-in, left, and DFG-out, right), showing only important structural features to make a simpler picture. The figure shows how the hinge region is conserved for all structures in both ensembles, while more variations can be observed for the DFG motif, especially in the «DFG-out» ensemble. Relatively, large variations are also observed for solvent exposed side chains of Glu546 and Lys627, especially in ensemble of DFG-out conformations.

The results of Trk ligands' docking with ensembles IN1-4 (left) and OUT1-4 (right) are listed in Table 5.

Bold numbers in Table 5 mark the GlideXP score minimum for each compound in each ensemble. Comparison of these scores appears to be useful to predict the most likely conformational state of the target kinase domain during the ligand binding event. Once again, the differences between DFG-in and DFG-out minima in the ensemble score are usually higher for inhibitors classified as type II, than for type I inhibitors. A few reportedly type I inhibitors have in our study lower minima for DFG-out-type II conformations than for DFG-in, which was also observed in previously described IFD studies. We found five compounds (**3**, **6**, **9**, **13**, **15**, **19**; Table 5) for which our IN–OUT prediction is not in agreement with literature [14].

To check the ability of the ensemble docking protocol to recover 151 Trk ligands (Dataset 2 in Section 2.2) from the larger combined database containing 151 Trk ligands and 1000 decoys (1K drug-like ligand decoys' set from Schrödinger [33], Dataset 3 in Section 2.2) an enrichment experiment was performed.

The distribution of ligands from both ligand sets, based on their GlideXP score obtained in the enrichment experiment, is shown in Table 6.

The Glide XP score was used as criteria for detection of actives from the large ligand pool. Any ligand was classified as active if its score was lower than −12.0 kcal/mol. It may be noted that ≈44% of ligands classified as DFG-in binders from the second ligand set (left, Table 6) have a GlideXP score below −12 kcal/mol, while no ligands classified as DFG-in binders from the third ligand set (right, Table 6) have such good score. As to DFG-out conformations, ≈26% of DFG-out binders from the second ligand set (left, Table 6) have a GlideXP score below −12 kcal/mol, while 3.8% of DFG-in binders from the third ligand set (right, Table 6) have a GlideXP score below −12 kcal/mol.

**Table 6**
The distribution of ligands from database of Trk ligands and decoy set regarding their Glide XP score.

| Target | Trk ligands Count per target | | Decoy set Count per target | |
|---|---|---|---|---|
| | Score < −12.0 | All | Score < −12.0 | All |
| IN1 | 9 | 15 | 0 | 82 |
| IN2 | 1 | 10 | 0 | 65 |
| IN3 | 7 | 12 | 0 | 49 |
| IN4 | 6 | 15 | 0 | 60 |
| OUT1 | 10 | 26 | 12 | 203 |
| OUT2 | 9 | 22 | 4 | 183 |
| OUT3 | 3 | 36 | 8 | 235 |
| OUT4 | 4 | 15 | 4 | 109 |

All—number of ligands found for target. Score < −12.0—number of ligands found for target that have GlideXP score bellow −12.0 kcal/mol.

We may conclude from these findings that virtual screening of random datasets gives a much lower probability to find a reasonable good binder for the DFG-in (active) conformation of Trk kinase receptor than for the DFG-out (inactive) form of the same kinase.

Finally, we noticed that the addition of a positive offset of 1.2 kcal/mol to all DFG-out scores improves the prediction of DFG-state using our strategy. Fig. 11A and B shows that after screening 10% of the combined database (Trk + decoys) using the Glide XP protocol (final stage of VSW) ≈45% of all Trk ligands were recovered. We observe that if a positive correction of DFG-out scores is applied the enrichment curves are closer to the ideal curve at low percentages of screened database (Fig. 11B) than in the case of uncorrected DFG-out scores (Fig. 11A).

## 4. Conclusions

The development of Trk-specific kinase inhibitors that can be used as possible medicaments against cancer and pain is an important research goal in various academic groups, as well as in pharmaceutical companies worldwide. We have found that homology modelling of TrkB receptor with YASARA followed by the induced fit docking (IFD) protocol proposed by Schrödinger is a valid tool for computational selection of initial hits. YASARA

was selected because of its user-friendliness, its relevance and its very well documented output. Two homology models produced by YASARA (one DFG-in and one DFG-out TrkB conformation) were selected for subsequent modelling and docking. These two models were then subjected to further re-modelling using an IFD protocol that takes into account receptor plasticity during the docking process. Several known ligands reported as type I or type II inhibitors were selected for the IFD experiment. They were tried for both DFG-in and DFG-out binding and the fit between experimental binding type and calculated score in the DFG-in and DFG-out model was checked. Analysis of the IFD results showed that they could be used with limited approximation for prediction of the activity range, and also for predicting the most favourable DFG conformational state of the kinase–ligand complex.

Since the IFD protocol is computationally intensive, it can be used only for limited number of ligands. To overcome this limitation ensemble docking with limited receptor plasticity was used for the screening of larger collections of compounds. Two ensembles were used, composed respectively of four representative DFG-in and four representative DFG-out receptor–ligand models obtained with IFD. Ensemble docking was performed with the same set of ligands used for IFD, and the results showed that also ensemble docking may be used for prediction of the DFG binding mode. An enrichment experiment also showed how ensemble docking may be useful for the identification of Trk ligands from a large combined (ligands + decoys) database.

Finally, we underline the extreme importance to take into account both DFG-in and DFG-out conformational states of TrkB to get more reasonable relationships between the docking score and experimental inhibition measured by $pIC_{50}$ for a given set of ligands.

## Acknowledgements

This work was supported by the FIRB program CHEMPROFARMANET-(RBPR05NWWC) and Slovenian Research Agency (ARRS) through Physical Chemistry Research Program P1-0201.

## Appendix A. Supplementary data

Supplementary data associated with this article can be found, in the online version, at doi:10.1016/j.jmgm.2010.09.008.

## References

[1] J. Soule, E. Messaoudi, C.R. Bramham, Brain-derived neurotrophic factor and control of synaptic consolidation in the adult brain, Biochem. Soc. Trans. 34 (2006) 600–604.
[2] S. Pezet, S.B. McMahon, Neurotrophins: mediators and modulators of pain, Annu. Rev. Neurosci. 29 (2006) 507–538.
[3] A. Patapoutin, L.F. Reichardt, Trk receptors: mediators of neurotrophin action, Curr. Opin. Neurobiol. 11 (2001) 272–280.
[4] S. Vepsalainen, E. Castren, S. Helisalmi, S. Iivonen, A. Mannermaa, M. Lehtovirta, T. Hanninen, H. Soininen, M. Hiltunen, Genetic analysis of BDNF and TrkB gene polymorphisms in Alzheimer's disease, J. Neurol. 252 (2005) 423–428.
[5] K. Schindowski, K. Belarbi, L. Buee, Neurotrophic factors in Alzheimer's disease: role of axonal transport, Genes Brain Behav. 7 (Suppl. 1) (2008) 43–56.
[6] C.J. Thiele, Z.J. Li, A.E. Mckee, On Trk-The TrkB signal transduction pathway is an increasingly important target in cancer biology, Clin. Cancer Res. 15 (2009) 5962–5967.
[7] G.M. Brodeur, Neuroblastoma: biological insights into a clinical enigma, Nat. Rev. Cancer 3 (2003) 203–216.
[8] G.M. Brodeur, J.E. Minturn, R. Ho, A.M. Simpson, R. Iyer, C.R. Varela, J.E. Light, V. Kolla, A.E. Evans, Trk receptor expression and inhibition in neuroblastomas, Clin. Cancer Res. 15 (2009) 3244–3250.
[9] A. Schramm, J.H. Schulte, K. Astrahantseff, O. Apostolov, V. van Limpt, H. Sieverts, S. Kuhfittig-Kulle, P. Pfeiffer, R. Versteeg, A. Eggert, Biological effects of TrkA and TrkB receptor signaling in neuroblastoma, Cancer Lett. 228 (2005) 143–153.
[10] M.K.Y. Siu, O.G.W. Wong, A.N.Y. Cheung, TrkB as a therapeutic target for ovarian cancer, Expert Opin. Ther. Targets 13 (2009) 1169–1178.
[11] C.W. Au, M.K. Siu, X. Liao, E.S. Wong, H.Y. Ngan, K.F. Tam, D.C. Chan, Q.K. Chan, A.N. Cheung, Tyrosine kinase B receptor and BDNF expression in ovarian cancers—effect on cell migration, angiogenesis and clinical outcome, Cancer Lett. 281 (2009) 151–161.
[12] A.T. Weeraratna, J.T. Arnold, D.J. George, A. DeMarzo, J.T. Isaacs, Rational basis for Trk inhibition therapy for prostate cancer, Prostate 45 (2000) 140–148.
[13] Y. Yu, S. Zhang, X. Wang, Z. Yang, G. Ou, Overexpression of TrkB promotes the progression of colon cancer, APMIS 118 (2010) 188–195.
[14] T. Wang, D. Yu, M.L. Lamb, Trk kinase inhibitors as new treatments for cancer and pain, Expert Opin. Ther. Pat. 19 (2009) 305–319.
[15] H. Berman, K. Henrick, H. Nakamura, Announcing the worldwide Protein Data Bank, Nat. Struct. Biol. 10 (2003) 980.
[16] Y. Liu, N.S. Gray, Rational design of inhibitors that bind to inactive kinase conformations, Nat. Chem. Biol. 2 (2006) 358–364.
[17] F. Zuccotto, E. Ardini, E. Casale, M. Angiolini, Through the "Gatekeeper Door": exploiting the active kinase conformation, J. Med. Chem. 53 (2010) 2681–2694.
[18] T. Wang, M.L. Lamb, D.A. Scott, H. Wang, M.H. Block, P.D. Lyne, J.W. Lee, A.M. Davies, H.J. Zhang, Y. Zhu, F. Gu, Y. Han, B. Wang, P.J. Mohr, R.J. Kaus, J.A. Josey, E. Hoffmann, K. Thress, T. Macintyre, C.A. Omer, D. Yu, Identification of 4-aminopyrazolylpyrimidines as potent inhibitors of Trk kinases, J. Med. Chem. 51 (2008) 4672–4684.
[19] S.H. Kim, J.S. Tokarski, K.J. Leavitt, B.E. Fink, M.E. Salvati, R. Moquin, M.T. Obermeier, G.L. Trainor, G.G. Vite, L.K. Stadnick, J.S. Lippy, D. You, M.V. Lorenzi, P. Chen, Identification of 2-amino-5-(thioaryl)thiazoles as inhibitors of nerve growth factor receptor TrkA, Bioorg. Med. Chem. Lett. 18 (2008) 634–639.
[20] B. Lippa, J. Morris, M. Corbett, T.A. Kwan, M.C. Noe, S.L. Snow, T.G. Gant, M. Mangiaracina, H.A. Coffey, B. Foster, E.A. Knauth, M.D. Wessel, Discovery of novel isothiazole inhibitors of the TrkA kinase: structure–activity relationship, computer modeling, optimization, and identification of highly potent antagonists, Bioorg. Med. Chem. Lett. 16 (2006) 3444–3448.
[21] E. Krieger, http://www.yasara.org, 2010.
[22] H. Venselaar, R.P. Joosten, B. Vroling, C.A.B. Baakman, M.L. Hekkelman, E. Krieger, G. Vriend, Homology modelling and spectroscopy, a never-ending love story, Eur. Biophys. J. 39 (2010) 551–563.
[23] H. Zhong, L.M. Tran, J.L. Stang, Induced-fit docking studies of the active and inactive states of protein tyrosine kinases, J. Mol. Graph Model. 28 (2009) 336–346.
[24] E. Krieger, K. Joo, J. Lee, S. Raman, J. Thompson, M. Tyka, D. Baker, K. Karplus, Improving physical realism, stereochemistry, and side-chain accuracy in homology modeling: four approaches that performed well in CASP8, Proteins 77 (Suppl. 9) (2009) 114–122.
[25] D.L. Shelton, J. Sutherland, J. Gripp, T. Camerato, M.P. Armanini, H.S. Phillips, K. Carroll, S.D. Spencer, A.D. Levinson, Human trks: molecular cloning, tissue distribution, and expression of extracellular domain immunoadhesins, J. Neurosci. 15 (1995) 477–491.
[26] The Universal Protein Resource (UniProt) in 2010, Nucleic Acids Res. 38 (2010) D142–D148.
[27] E. Jain, A. Bairoch, S. Duvaud, I. Phan, N. Redaschi, B.E. Suzek, M.J. Martin, P. McGarvey, E. Gasteiger, Infrastructure for the life sciences: design and implementation of the UniProt website, BMC Bioinformatics 10 (2009) 136.
[28] R. Apweiler, A. Bairoch, C.H. Wu, Protein sequence databases, Curr. Opin. Chem. Biol. 8 (2004) 76–80.
[29] S.F. Altschul, T.L. Madden, A.A. Schaffer, J. Zhang, Z. Zhang, W. Miller, D.J. Lipman, Gapped BLAST and PSI-BLAST: a new generation of protein database search programs, Nucleic Acids Res. 25 (1997) 3389–3402.
[30] R.D. King, M.J. Sternberg, Identification and application of the concepts important for accurate and reliable protein secondary structure prediction, Protein Sci. 5 (1996) 2298–2310.
[31] S.R. Hubbard, Crystal structure of the activated insulin receptor tyrosine kinase in complex with peptide substrate and ATP analog, EMBO J. 16 (1997) 5572–5581.
[32] S. Patnaik, K.L. Stevens, R. Gerding, F. Deanda, J.B. Shotwell, J. Tang, T. Hamajima, H. Nakamura, M.A. Leesnitzer, A.M. Hassell, L.M. Shewchuck, R. Kumar, H.S. Lei, S.D. Chamberlain, Discovery of 3,5-disubstituted-1H-pyrrolo[2,3-b]pyridines as potent inhibitors of the insulin-like growth factor-1 receptor (IGF-1R) tyrosine kinase, Bioorg. Med. Chem. Lett. 19 (2009) 3136–3140.
[33] Schrödinger LLC., http://www.schrodinger.com, 2010.
[34] S. Rao, P.C. Sanschagrin, J.R. Greenwood, M.P. Repasky, W. Sherman, R. Farid, Improving database enrichment through ensemble docking, J. Comput. Aided Mol. Des. 22 (2008) 621–627.
[35] T.A. Halgren, R.B. Murphy, R.A. Friesner, H.S. Beard, L.L. Frye, W.T. Pollard, J.L. Banks, Glide: a new approach for rapid, accurate docking and scoring. 2. Enrichment factors in database screening, J. Med. Chem. 47 (2004) 1750–1759.
[36] W. Sherman, T. Day, M.P. Jacobson, R.A. Friesner, R. Farid, Novel procedure for modeling ligand/receptor induced fit effects, J. Med. Chem. 49 (2006) 534–553.
[37] R.A. Friesner, J.L. Banks, R.B. Murphy, T.A. Halgren, J.J. Klicic, D.T. Mainz, M.P. Repasky, E.H. Knoll, M. Shelley, J.K. Perry, D.E. Shaw, P. Francis, P.S. Shenkin, Glide: a new approach for rapid, accurate docking and scoring. 1. Method and assessment of docking accuracy, J. Med. Chem. 47 (2004) 1739–1749.
[38] Amgen Inc., Heteroaryl-substituted alkyne compounds and methods of use, WO2006044823, 2006.

[39] AstraZeneca AB, AstraZeneca UK Limited, Pyrazole derivates as inhibitors of receptor tyrosine kinases, WO2005049033, 2005.
[40] R. Tripathy, T.S. Angeles, S.X. Yang, J.P. Mallamo, TrkA kinase inhibitors from a library of modified and isosteric Staurosporine aglycone, Bioorg. Med. Chem. Lett. 18 (2008) 3551–3555.
[41] Bristol-Myers Squibb Company, Pyrrolotriazine kinase inhibitors, WO2007061882, 2007.
[42] S. Knapper, A.K. Burnett, T. Littlewood, W.J. Kell, S. Agrawal, R. Chopra, R. Clark, M.J. Levis, D. Small, A phase 2 trial of the FLT3 inhibitor lestaurtinib (CEP701) as first-line treatment for older patients with acute myeloid leukemia not considered fit for intensive chemotherapy, Blood 108 (2006) 3262–3270.
[43] P. Revill, N. Serradell, J. Bolos, E. Rosa, Lestaurtinib—multikinase inhibitor, oncolytic, antipsoriatic agent, Drug Future 32 (2007) 215–222.